ISBN: 978-3-95450-227-1 ISSN: 2673-5490 doi:10.18429/JACoW-IPAC2022-THPOST040

COMMISSIONING OF AN X-BAND CAVITY FOR LONGITUDINAL PHASE SPACE LINEARIZATION AT UCLA PEGASUS LABORATORY *

P. Denham †, A. Ody, P. Musumeci
Department of Physics and Astronomy
University of California at Los Angeles, Los Angeles, CA, USA

Abstract

This paper discusses the commissioning of an X-band (9.6 GHz) linearizer cavity at the UCLA PEGASUS beamline. The photoinjector gun and booster linac operate at S-band (2.856 GHz) and the linearizer cavity can be used to compensate temporally correlated energy spread inherited by the use of relatively long (many ps) laser pulses at the photocathode. The cavity is comprised of 7 cells for a total length of a 9.45 cm, and is installed in the drift section between the gun and the linac. It can be used to remove higher order correlations and minimize the beam energy spread of 13 ps long beams to 10^{-4}.

INTRODUCTION

Linearizing the longitudinal phase space (LPS) of electron beams generated in RF-photoinjectors is essential for pushing the limits of ultrafast electron diffraction (UED) and ultrafast electron microscopy (UEM) [1]. UED sources that rely on velocity bunching benefit from having additional cavities because they can be utilized to remove higher-order distortions that show up at the ballistic focus, which can yield sub fs pulses. On the other hand, UEM sources favor ps long Cigar beams with low energy spread (<10^{-4}), as they have demonstrated an ideal compromise between temporal and spatial resolution (10 ps–10 nm) [2, 3].

Extensive work has been done, using multiple cavities of the same frequency for LPS linearization for both UED and UEM applications. Multi-objective optimizations of injectors with several cavities can feasibly generate attosecond pulses when operated in stroboscopic mode [4]. Alternatively, the pairing of an RF-gun and buncher LINAC has shown capable of linearizing either the bunching process or energy spread [5].

We focus on using a single higher harmonic X-band cavity for LPS linearization to reduce energy spread at the PEGASUS beamline. First, we provide design details and measurements of the X-band Cavity shunt impedance, then amplitude and phase stability. Then the LPS linearization procedure is described. Finally, we present results of energy spread minimization at the PEGASUS beam line that were obtained by using a high resolution (1.1 m dispersion) spectrometer.

* Work supported by DOE STTR grant No. DE-SC0013115 and by by the National Science Foundation under STROBE Science and Technology Center Grant No. DMR-1548924.
† pdenham@physics.ucla.edu

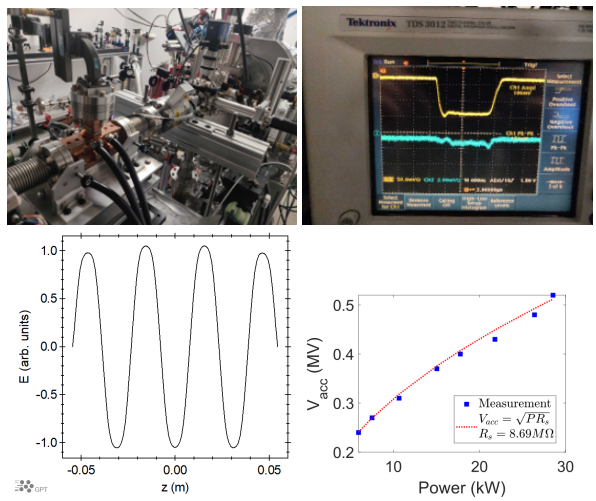

Figure 1: (a) X-band cavity installation at PEGASUS. (b) Forward and reverse power measurements. (c) Longitudinal Field profile. (d) Shunt Impedance measurement.

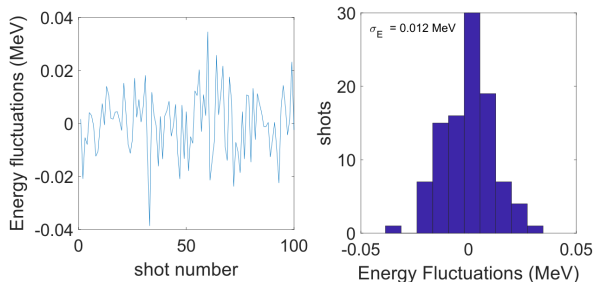

Figure 2: Measured central energy fluctuations at cavity zero crossing.

X-BAND CAVITY CHARACTERIZATION

The X-band linearizer is a 7 cell X-band (9.6 GHz) accelerating cavity that removes the higher order longitudinal phase space correlations and suppresses energy spread for ultra-fast electron microscopy. Each cell in the cavity is 13.492 mm (9.45 cm total length), and has a side-coupled geometry with noses. The Noses were added to increase accelerating voltage. The Beam pipe radius is 4 mm. The relative phase velocity of the structure is $\beta = 0.9922$ (ideally corresponding to a 3.5 MeV beam). There is a 30 MHz mode separation between accelerating and neighboring modes. The design shunt impedance is 90 MΩ/m. We installed the cavity 1.1 m

ISBN: 978-3-95450-227-1 ISSN: 2673-5490 doi:10.18429/JACoW-IPAC2022-THPOST040

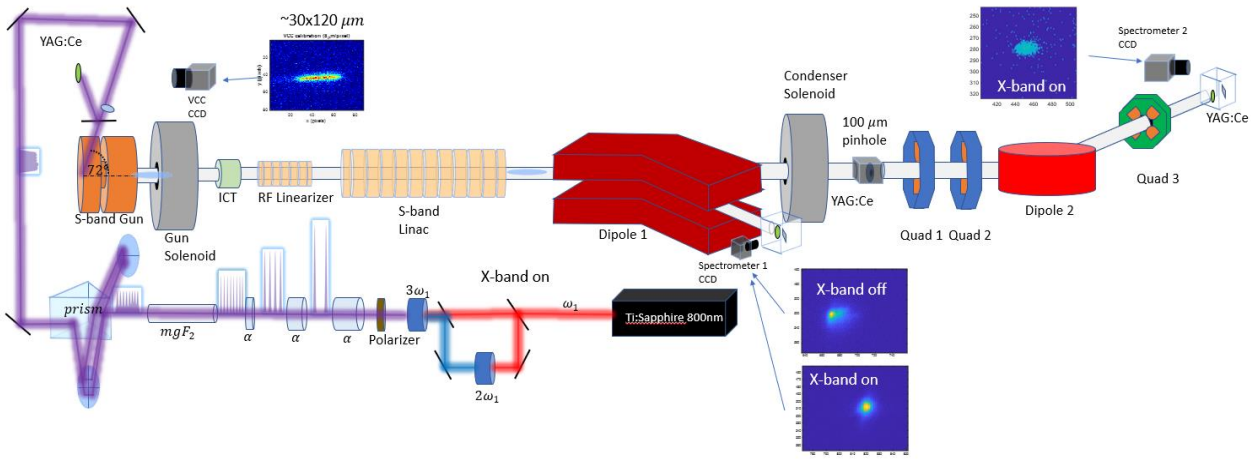

Figure 3: Schematic of Beamline Layout for energy spread compensation measurements.

downstream of the cathode, which is also 0.5m upstream of the linac entrance. The cavity installation and forward and reverse power measurements are shown in Fig. 1 (top left and right panels, respectively). The longitudinal field profile is shown (bottom left panel).

The cavity frequency of 9.6 GHz is chosen to facilitate synchronization with the 1.6 cell S-Band photogun and 11-cell S-Band LINAC cavity on the PEGASUS beamline. The low-level 2.856 GHz RF seed that is used to drive the S-Band klystron has a portion split of first to be frequency divided by 36 down to 79.33 MHz, with part of the signal as an input to the Sycnhrolock system to synchronize with the Ti:Sapphire laser system. The remaining low level signal is then frequency multiplied up by 121 to achieve a nominal frequency of 9.599 GHz that is phaselocked with the low level RF, which is then preamplified and sent to our X-band klystron.

We measured the shunt impedance of the cavity by measuring accelerating voltage amplitude (relative to the zero crossing phase) on the first spectrometer screen for different cavity input power set points. We find a shunt impedance of 8.69 MΩ to be in good agreement with the design (bottom right panel of Fig. 1). At the maximum power set point of 30 kW, the peak field in the cavity is 10 MV/m.

Next we assessed the amplitude and phase stability in operation. To quantify amplitude stability, we set the X-band to the maximum accelerating phase. At this set point, the centroid energy gain is described by the taylor expansion of $\Delta\gamma = \alpha_X \cos(\delta\phi) \approx \alpha_X(1 - \delta\phi^2/2)$, where $\delta\phi$ is a small phase offset. In this scenario, the centroid energy is an excellent proxy for amplitude fluctuations because the dependence on phase is second order. The statistics from 100 shots indicate the amplitude stability of the X-band is 2×10^{-3}. On the other hand, the deviations of centroid energy at the zero crossing phase are linear with phase fluctuations, i.e., $\delta\gamma = \alpha_X \sin(\delta\phi) \approx \alpha_X\delta\phi$. The energy deviations were collected at the zero crossing phase over a 100 shots. They are shown in Fig. 2. After dividing the rms energy deviations $\sigma_E = 0.012MeV$ by the cavity voltage, we obtain an estimate of phase fluctuations, $\Delta\phi = 1.2°$. This level of phase fluctuations is tolerable in the energy spread compensation.

LONGITUDINAL PHASE SPACE LINEARIZATION

The experimental layout for LPS linearization is shown in Fig. 3. Correlations imparted on the longitudinal phase space by a S-band gun, S-band LINAC, and the X-band linearizer can be obtained by integration. To estimate what degree of compensation is obtainable, we assume all cavities are set to maximum accelerating/decelerating phases. In that case, the relation between energy and time is given by:

$$\gamma(t) = \gamma_0 \cos(2\pi f_0 t) - \gamma_x \cos(2\pi f_X t) + \gamma_L \cos(2\pi f_0 t) \quad (1)$$

where t, is the time of arrival relative to the resonant particle, γ_0, γ_L, γ_x, are normalized accelerating voltages of the S-band gun, Linac, and x-band linearizer, respectively. The cavity angular frequencies f_0, f_X are $2.856GHz$, and $9.6GHz$ respectively. If $\gamma_x = (\gamma_0 + \gamma_L)f_0^2/f_X^2$, then the quadratic correlation in the Taylor expansion of Eq. (1) vanishes. If we neglect space charge effects, then an initial 10 ps flat-top distribution can achieve an RMS relative energy spread of $\sigma_\gamma/\gamma \approx 10^{-5}$. To further exemplify the process, the results of a start-to-end simulation of the PEGASUS beamline are shown in Fig. 4. The longitudinal phase space is quadratic before the X-band is activated, then becomes flat with a narrow projection of 2×10^{-5} along the relative energy axis after activation. In a typical injector operation, the gun imparts linear chirp, which must also be compensated.

To experimentally achieve the aforementioned degree of compensation we first worked to reshape and stretch our 40 fs RMS Gaussian temporal profile into 13.3 ps flat top shape at the cathode by using 3 α-BBO crystals with respective lengths 8.7 5mm, 4.375 mm, 2.1875 mm. Then a MgF_2 crystal and a prism were utilized to smear the temporal profile. Next, preliminary laser pulse characterization was done using spectrometer 1, with the gun phase set to 30 degrees. The

ISBN: 978-3-95450-227-1 ISSN: 2673-5490 doi:10.18429/JACoW-IPAC2022-THPOST040

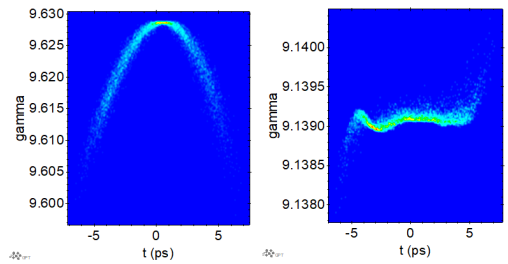

Figure 4: GPT simulation of longitudinal phase space linearization before (left panel) and after (right panel) compensation of the longitudinal phase space by the X-band cavity.

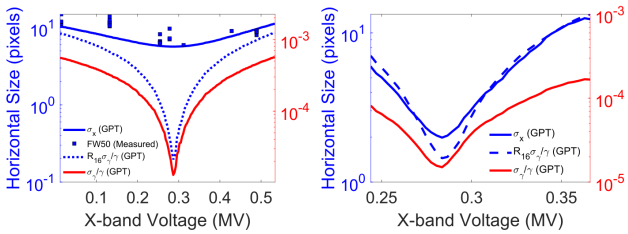

Figure 5: (Left) Simulated and measured spectrometer 1 screen beam size (solid) with respect to the accelerating voltage for optimum phase; the energy spread's contribution to beamsize (dashed). Expected energy spread is plotted on the right axis in red. (Right) Simulated spectrometer 2 beam size and energy spread.

introduction of the MgF_2 crystal and prism on the laser path smoothed out density modulations on spectrometer screen.

Resolving energy spread below 10^{-4} requires nm-scale normalized emittances. To minimize the emittance, we focused the drive laser (266 nm) onto a NaKSb photocathode [6] by utilizing a 72∘ oblique incidence vacuum port and a final focus lens (f = 175 mm) mounted on a translation stage. The oblique port allows the final lens to be brought closer to the cathode surface [7], but makes the initial spot to be asymmetric. A potential drawback is that the gun solenoid couples the larger of the two projected emittances into the horizontal plane at the spectrometer screen.

The linac was tuned to the off-crest accelerating phase, compensating for the initially imparted linear correlation between time and energy; then, a purely quadratic correlation between time and energy remained. Finally, the X-band was tuned to the decelerating phase, the gun solenoid was set to minimize the beta function at the spectrometer screen, then we scanned the X-band cavity amplitude. The beamsize reached a minimum. It was reduced by a factor of 2, from 300 µm to 150 µm, as shown in the bottom left panel of Fig. 5. We performed GPT simulations of the experimental scan. The results are superimposed with experimental data in the bottom left panel of Fig. 5, where the horizontal beam size is plotted along with the contribution from the energy spread to the final screen size as a function of the X-band cavities voltage. The corresponding relative energy spread is shown in red and contributes less than a pixel when the

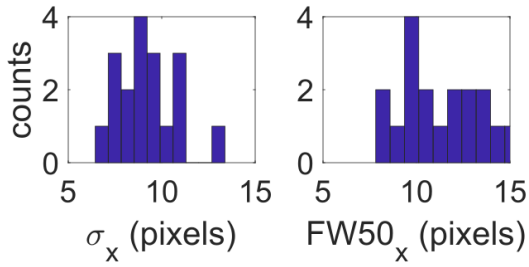

Figure 6: Spectrometer 2 sample image statistics for 20 shots.

energy spread is $< 10^{-4}$. The figure shows that our ability to resolve the actual energy spread was limited by the emittance contributions to the beam size at spectrometer 1.

The next experimental phase is focused on improving resolution in the second dispersion section illustrated in Fig. 3. The main improvements come from adding a 100 µm pinhole and a horizontally defocusing qadrupole in the final dispersion arm. The pinhole reduces the contribution to the measured beam size from the horizontal emittance (at the cost of charge transmission). Meanwhile, the final quad increases the dispersion coefficient. Typically, for a final dispersion length L, dipole bend radius ρ and bend angle θ the dispersion is denoted by $R_{16} = \rho(1-\cos(\theta)) + L\sin(\theta)$. In the thin lens approximation, if a defocusing lens with focal length f is positioned in the dispersion arm between the dipole and the screen such that it maximizes dispersion, then the expression characterizing dispersion becomes:

$$\tilde{R}_{16} = R_{16}\left(1 + \frac{L + \rho\tan(\theta/2)}{4f}\right) \quad (2)$$

With these additions, spectrometer 2's dispersion exceeds $1m$ when the final quadrupole is fully powered. Shown in the bottom right panel of Fig. 5, we find these enhancements enable there to be a linear relationship between energy spread and beam size at the detector screen for relative spreads below 5×10^{-5}. Initial measurements taken on spectrometer 2 are shown in Fig. 6. We find that the measured beam sizes correspond to energy spread within an order unity factor of 10^{-4}.

FUTURE DIRECTION

An X-band harmonic linearizer cavity has been installed at the PEGASUS beamline and is currently being commissioned. So far, preliminary energy spread compensation measurements have been taken. Energy spread has been reduced below the transverse emittance resolution limit at the first spectrometer. A more comprehensive analysis of the dependence on arrival time to phase, and amplitude stability is envisioned. In the interim, we will work on improving beam pointing stability at spectrometer 2 pinhole for future energy spread measurements. We plan to utilize the X-band Cavity in future UEM experiments.

ISBN: 978-3-95450-227-1 ISSN: 2673-5490 doi:10.18429/JACoW-IPAC2022-THPOST040

REFERENCES

[1] P. Musumeci *et al.*, "Advances in bright electron sources", *Nuclear Instruments and Methods in Physics Research Section A: Accelerators, Spectrometers, Detectors and Associated Equipment*, vol 907, pp. 209-220, 2018. doi:10.1016/j.nima.2018.03.019

[2] R. Li and P. Musumeci, "Single-shot MeV transmission electron microscopy with picosecond temporal resolution", *Physical Review Applied*, vol 2, no. 2, p. 024003, 2014. doi:10.1103/PhysRevApplied.2.024003

[3] P. Denham and P. Musumeci, "Space-Charge Aberrations in Single-Shot Time-Resolved Transmission Electron Microscopy", *Phys. Rev. Applied*, vol. 15, p. 024050, 2021. doi:10.1103/PhysRevApplied.15.024050

[4] Adam Bartnik *et al.*, "Ultimate bunch length and emittance performance of an MeV ultrafast electron diffraction apparatus with a DC gun and a multi-cavity SRF linac, 2021. doi:10.48550/arXiv.2108.06414

[5] B. Zeitler, K. Floettmann, and F. Gruner, " Linearization of the longitudinal phase space without higher harmonic field", *in Physical Review Special Topics - Accelerators and Beams*, vol. 18, p.120102, 2015. doi:10.1103/physrevstab.18.120102

[6] C. A. Pennington *et al.*, "Alkali Antimonide Photocathode Characterization in a High Gradient S-Band Gun", presented at IPAC'22, Bangkok, Thailand, Jun. 2022, paper THPOST044, this conference.

[7] J. Maxson, D. Cesar, G. Calmasini, A. Ody, P. Musumeci, and D. Alesini, "Direct measurement of sub- 10 fs relativistic electron beams with ultralow emittance", *Physical review letters*, vol. 118, p. 154802, 2017. 10.1103/PhysRevLett.118.154802